Spatial correlation of action potential duration and diastolic dysfunction in transgenic and drug-induced LQT2 rabbits

Katja E. Odening, MD,[*] Bernd A. Jung, PhD,[†] Corinna N. Lang, MD,[*] Rocio Cabrera Lozoya, MSc,[‡] David Ziupa, MD,[*] Marius Menza, MSc,[†] Jatin Relan, PhD,[‡] Gerlind Franke, PhD,[*] Stefanie Perez Feliz,[*] Gideon Koren, MD,[§] Manfred Zehender, MD,[*] Christoph Bode, MD,[*] Michael Brunner, MD,[*] Maxime Sermesant, PhD,[‡] Daniela Föll, MD[*]

From the [*]Department of Cardiology and Angiology I, Heart Center Freiburg University, Freiburg, Germany, [†]Department of Radiology, Medical Physics, University Hospital Freiburg, Freiburg, Germany, [‡]INRIA, Asclepios Research Project, Cardiac Modelling, Sophia Antipolis, France, and [§]Division of Cardiology, Cardiovascular Research Center, Rhode Island Hospital, Alpert Medical School of Brown University, Providence, Rhode Island.

BACKGROUND Enhanced dispersion of action potential duration (APD) is a major contributor to long QT syndrome (LQTS)-related arrhythmias.

OBJECTIVE To investigate spatial correlations of regional heterogeneities in cardiac repolarization and mechanical function in LQTS.

METHODS Female transgenic LQTS type 2 (LQT2; n = 11) and wild-type littermate control (LMC) rabbits (n = 9 without E4031 and n = 10 with E4031) were subjected to phase contrast magnetic resonance imaging to assess regional myocardial velocities. In the same rabbits' hearts, monophasic APDs were assessed in corresponding segments.

RESULTS In LQT2 and E4031-treated rabbits, APD was longer in all left ventricular segments ($P < .01$) and APD dispersion was greater than that in LMC rabbits ($P < .01$). In diastole, peak radial velocities (Vr) were reduced in LQT2 and E4031-treated compared to LMC rabbits in LV base and mid (LQT2: -3.36 ± 0.4 cm/s, $P < .01$; E4031-treated: -3.24 ± 0.6 cm/s, $P < .0001$; LMC: -4.42 ± 0.5 cm/s), indicating an impaired diastolic function. Regionally heterogeneous diastolic Vr correlated with APD (LQT2: correlation coefficient [CC] 0.38, $P = .01$; E4031-treated: CC 0.42, $P < .05$). Time-to-diastolic peak Vr were prolonged in LQT2 rabbits (LQT2: 196.8 ± 2.9 ms, $P < .001$; E4031-treated: 199.5 ± 2.2 ms, $P < .0001$, LMC 183.1 ± 1.5), indicating a prolonged contraction duration. Moreover, in transgenic LQT2 rabbits, diastolic time-to-diastolic peak Vr correlated with APD (CC 0.47, $P = .001$). In systole, peak Vr were reduced in LQT2 and E4031-treated rabbits

($P < .01$) but longitudinal velocities or ejection fraction did not differ. Finally, random forest machine learning algorithms enabled a differentiation between LQT2, E4031-treated, and LMC rabbits solely based on "mechanical" magnetic resonance imaging data.

CONCLUSIONS The prolongation of APD led to impaired diastolic and systolic function in transgenic and drug-induced LQT2 rabbits. APD correlated with regional diastolic dysfunction, indicating that LQTS is not purely an electrical but an electromechanical disorder.

KEYWORDS Long QT syndrome; Rabbits; Repolarization; Diastolic function; Cardiac electrophysiology; Cardiac MRI

ABBREVIATIONS APD = action potential duration; **APD$_{75}$** = action potential duration at 75% of repolarization; **[Ca^{2+}]$_i$** = cytoplasmic Ca^{2+} concentration; **CC** = correlation coefficient; **ECG** = electrocardiogram; **EPS** = electrophysiological study; **I$_{Ca,L}$** = L-type Ca2+ current; **I$_{Kr}$** = rapid delayed rectifier potassium current; **IV** = intravenously; **LMC** = wild-type littermate control; **LQT2** = long QT syndrome type 2; **LQTS** = long QT syndrome; **LV** = left ventricle/ventricular; **MAP** = monophasic action potential; **MRI** = magnetic resonance imaging; **pVT** = polymorphic ventricular tachycardia; **QTc** = heart-rate corrected QT; **SD** = standard deviation; **TTP** = time-to-peak velocities; **Vr** = radial velocities; **Vr_dia** = diastolic peak radial velocities; **Vz** = long-axis velocities; **Vz_dia** = diastolic peak long-axis velocities

Introduction

The inherited long QT syndrome (LQTS) is an arrhythmogenic disease characterized by impaired cardiac repolarization that clinically manifests with QT prolongation, polymorphic ventricular tachycardia (pVT), syncopes, and sudden cardiac death.[1] A spatially heterogeneous prolongation of repolarization leading to an enhanced dispersion of action potential duration (APD) is considered a major contributor to LQT-related arrhythmias.[2] As a result of their prolonged repolarization, patients with LQTS have globally prolonged cardiac contraction duration with transmural differences.[3,4] However, the spatial relationship between electrical and mechanical (dys)function remains to be elucidated.

Phase contrast magnetic resonance imaging (MRI) has been used successfully to determine regional differences in myocardial contraction and relaxation velocities in human patients.[5] Healthy women, who physiologically have longer repolarization than men, have altered peak velocities and different regional patterns of relaxation compared to men,[6] suggesting that it may be possible to determine changes and spatial differences in mechanical function in LQTS by using this technique.

Rabbits exhibit pronounced similarities in the expression and function of voltage-gated K^+ channels[7] and Ca^{2+} cycling proteins[8] as humans, suggesting that rabbits can fairly appropriately mimic the human phenotype of cardiac diseases with electrical and/or mechanical impairment. Indeed, several transgenic rabbit models of human diseases such as LQTS and hypertrophic cardiomyopathy have demonstrated pronounced similarities with the human phenotype.[9,10] Transgenic LQTS type 2 (LQT2) rabbits mimic human LQTS with QT prolongation, pVT, sudden cardiac death, and an increased APD dispersion as major arrhythmogenic mechanism.[9] Moreover, despite some species differences in myocardial motion between humans and small animals, we could recently show similarities between humans and rabbits in regional contractile behavior with a similar rotational motion,[11] indicating that LQT2 rabbits may be a useful tool to assess mechanical function in LQTS.

By using in vivo phase contrast MRI, ex vivo monophasic action potential (MAP) measurements, and machine learning approaches, we aimed at elucidating the spatial relationship between regional electrical and mechanical cardiac function and their spatial dispersion in transgenic and drug-induced LQT2 rabbits.

Methods

A more detailed method description can be found in the Online Supplement.

Rabbits

Adult female transgenic LQT2 (HERG-G628S, 4.1 ± 0.6 months, 2.4 ± 0.3 kg) and wild-type littermate control (LMC) rabbits (without drugs, 6.3 ± 1.0 months, 3.8 ± 0.6 kg; with E4031, 4.0 ± 0.2 months, 2.9 ± 0.3 kg) were subjected to MRI followed by MAP measurements.

Phase contrast MRI

To assess myocardial velocities, transgenic LQT2 (n = 11) and LMC rabbits (n = 9 without drugs, n = 10 with E4031, bolus 10 μg/kg and infusion 1 μg/(kg · min)[12]) were subjected to phase contrast MRI at 1.5 T (Avanto, Siemens, Germany).[11] Animals were anesthetized with (S)-ketamine/xylazine (12.5/3.75 mg/kg intramuscularly, followed by 1–2.5 mL/kg/h intravenously [IV]), which does not affect cardiac repolarization,[13] and positioned in a 12-channel head coil.

Experiments were performed with a black blood prepared gradient echo sequence with prospective electrocardiographic (ECG) gating and high temporal (7.6 ms) and spatial resolution (1.0 × 1.2 × 4 mm).[11] For data postprocessing, customized MATLAB software was used. For regional analysis, the left ventricle (LV) was partitioned into 16 segments in the base, mid, and apex (the American Heart Association model[14]). Mean radial (Vr) and long-axis (Vz) systolic and diastolic peak and time-to-peak (TTP) were determined. The standard deviation (SD) of TTP from 16 segments was calculated as a measure for mechanical dispersion. Heart rate-corrected diastolic TTP were computed as the percentage of RR.

MAP measurements in Langendorff-perfused rabbit hearts

To correlate electrical and mechanical function, MAPs were acquired in the same LQT2 (n = 10) and LMC rabbits (n = 9 without drugs; n = 10 with E4031; 0.1 μM[15]). Rabbits were anesthetized with (S)-ketamine/xylazine (12.5/3.75 mg/kg) intramuscularly and received 1000 IU heparin IV. After euthanasia with sodium thiopental (40 mg/kg) IV, hearts were excised rapidly and mounted on the Langendorff-perfusion setup (IH5, Hugo Sachs Electronic-Harvard Apparatus, Hugstetten, Germany). Hearts were retrogradely perfused with modified Krebs-Henseleit solution.[16] ECG, MAP, coronary flow, and pressures were continuously recorded with Isoheart software (Hugo Sachs Electronic, Version 1.1.1.218(32)).

After mechanical atrioventricular node ablation, hearts were stimulated with 2, 3, and 4 Hz to obtain APD at heart rates comparable to MRI (130–189 beats/min). Four MAP electrodes were repetitively positioned on all different LV segments except for the septal segments (see the Online Supplemental Figure 2). APDs at 75% of repolarization (APD$_{75}$) and standard deviations (SD) of APD$_{75}$ within all LV segments were calculated as measures for electrical dispersion.

Machine learning for image-based classification

Multivariate data analyses were performed by using random forest machine learning algorithms to explore the possibility to differentiate between LQT2, E4031-treated, and LMC rabbits based on MRI data. Image-based features included peak velocities, TTP, regional velocity statistics, and correlations with normal velocity curves (over 700 features per rabbit). Feature space dimension reduction was performed by using the χ^2 test. Only top-relevant features were considered. Cross-validation was used to obtain an estimate of classifier accuracy.[17]

Since heart-rate corrected QT (QTc) duration[18] and QT dispersion[19] are known arrhythmogenic risk factors in LQTS and since we observed correlations between APD and diastolic dysfunction in LQT2 rabbits, we next tested whether MRI can provide sufficient information to discern differences in the extent of APD prolongation by using random forest machine learning algorithms. LQT2 rabbits were divided into 2 groups: (1) rabbits with "very long" APD and "pronounced" dispersion (longest APD ≥ 155 ms,

SD_APD > 12 ms) and (2) rabbits with "long" APD and "moderate" dispersion (longest APD ≥ 140 ms and ≤ 155 ms, SD_APD ≤ 12 ms) (see the Online Supplemental Table 1).

Statistical analysis

For normally distributed values, we used the unpaired Student t test for comparisons and Pearson test for correlations. For values not normally distributed, we used the Mann-Whitney test for comparisons and Spearman test for correlations. Correlations were visualized by using linear least-squares fit calculated on the basis of all LQT2 rabbits' data. Analyses were performed with Prism 4.03 (Graphpad, San Diego, CA).

Results

Dispersion of cardiac repolarization in transgenic and drug-induced LQT2 rabbits

As shown in representative MAPs of the LV base of individual transgenic LQT2 and LMC rabbits (Figure 1B) and in averaged bull's eye plots of APD$_{75}$ in all LV regions (Figure 1C), LQT2 and E4031-treated rabbits had significantly longer APDs than did LMC rabbits. Moreover, the spatial dispersion of APD was significantly greater in LQT2 and E4031-treated rabbits than in LMC rabbits (Figure 1D). A similar difference was observed in surface ECG with significantly longer QT intervals in LQT2 and E4031-treated rabbits than in LMC rabbits (Figure 1E).

During faster stimulation, APD shortened in all groups (LQT2: $P < .0001$; E4031-treated: $P = .002$; LMC: $P = .002$). Despite this rate-dependent APD shortening, APD remained significantly longer in LQT2 and E4031-treated rabbits than in LMC rabbits at 3 Hz (3 Hz, base, LQT2, 132 ± 8.5 ms, $p = .02$; E4031-treated, 121 ± 3.6 ms $p = .04$; LMC, 113 ± 1; 4 Hz, LQT2, 105 ± 9.7, E4031, 97 ± 7.6 LMC, 89 ± 0.5). Moreover, APD dispersion remained more pronounced in LQT2 and E4031-treated rabbits than in LMC rabbits at 3 and 4 Hz (Figure 1D).

Mechanical function in transgenic and drug-induced LQT2 rabbits

Global peak systolic radial velocities (Vr) were significantly reduced in LQT2 and E4031-treated rabbits compared to LMC in LV base (LQT2: $P = .01$; E4031-treated: $P = .0004$) and mid (LQT2: $P = .002$; E4031-treated: $P = .0009$) and tended to be reduced in the apex (LQT2: $P = .07$) owing to regionally reduced velocities in anterior and anteroseptal segments (Figure 2A). Global peak systolic longitudinal velocities (Vz) did not differ. Regional systolic Vz, however, were reduced only in LQT2 in anteroseptal segments (Figure 2B). Ejection fractions were normal in all groups (Figure 2C). LV end-diastolic and end-systolic volumes were lower in the smaller LQT2 rabbits (Figure 2D). After body-weight correction, however, no differences were found between groups (Figure 2D).

Global and regional peak diastolic Vr were significantly reduced in LQT2 and E4031-treated rabbits in the LV base (LQT2: $P = .002$; E4031-treated: $P < .0001$), mid (LQT2: $P = .002$; E4031-treated: $P < .0001$), and apex (LQT2: $P = .01$; E4031-treated: $P = .006$; Figures 3A and 3B), indicating an impaired diastolic function in LQT2 rabbits. Global peak diastolic Vz did not differ between LQT2 and LMC rabbits, but were reduced in E4031-treated rabbits (base: $P < .0001$; mid: $P = .0002$; apex: $P = .02$). Regional diastolic Vz were reduced in LQT2 rabbits in anterior segments, while in E4031-treated rabbits, diastolic Vz were reduced in inferior and lateral regions (Figure 3D).

Global and segmental time-to-diastolic peak Vr (TTP_dia_Vr) were significantly longer in LQT2 and E4031-treated rabbits than in LMC rabbits (LQT2: base, $P = .0002$; mid, $P = .04$; E4031-treated: base, $P < .0001$, mid, $P < .0001$; Figure 4A), indicating a delayed relaxation due to prolonged contraction duration. After heart-rate correction, differences between LQT2 and LMC rabbits were even more pronounced (TTP_dia_Vr_base_%; LQT2: 65.2% ± 0.8%; LMC: 58.8% ± 0.6%; $P < .0001$; Figure 4B). In contrast, global and segmental heart-rate corrected TTP_dia_Vz were similar in all groups.

Correlation of electrical and mechanical dysfunction

In LQT2 rabbits, APD correlated moderately with the regional reduction in diastolic Vr and Vz in the LV base (Vr_dia: correlation coefficient [CC] 0.38, $P = .02$; Vz_dia: CC 0.47, $P = .002$; Figure 3C). Moreover, the SD of APD and peak diastolic Vr, as markers of electrical/mechanical dispersion, correlated strongly in the LV mid (CC 0.75, $P = .03$). In addition, TTP_dia_Vr, as a marker of contraction duration, correlated moderately with APD in the LV base (TTP_dia_Vr: CC 0.47, $P = .001$; TTP_dia_Vr_%: CC 0.43, $P = .001$; Figure 4D). As for systolic function, APD correlated moderately with systolic Vz in the LV mid (CC 0.37, $P = .03$). In E4031-treated rabbits, APD correlated with diastolic Vr (CC 0.42, $P = .04$), while in LMC rabbits, no correlations were observed.

Machine learning approaches for MRI-based classification

On the basis of the observed differences in mechanical function, we first explored the possibility to differentiate between groups solely based on "mechanical" phase contrast MRI data. By using random forest machine learning algorithms with only most relevant features (see the Online Supplemental Table 2), we could differentiate between LQT2 and LMC rabbits with an accuracy of 95%. All LQT2 rabbits were correctly classified, while 1 LMC with relatively low Vr_dia was misclassified (see the Online Supplemental Table 3). Most relevant features were regional diastolic Vr, TTP_dia_Vr, and their SDs (see the Online Supplemental Table 2), while systolic features were only of minor importance. As indicated in the cumulative region relevance plot, important features were mainly located in the
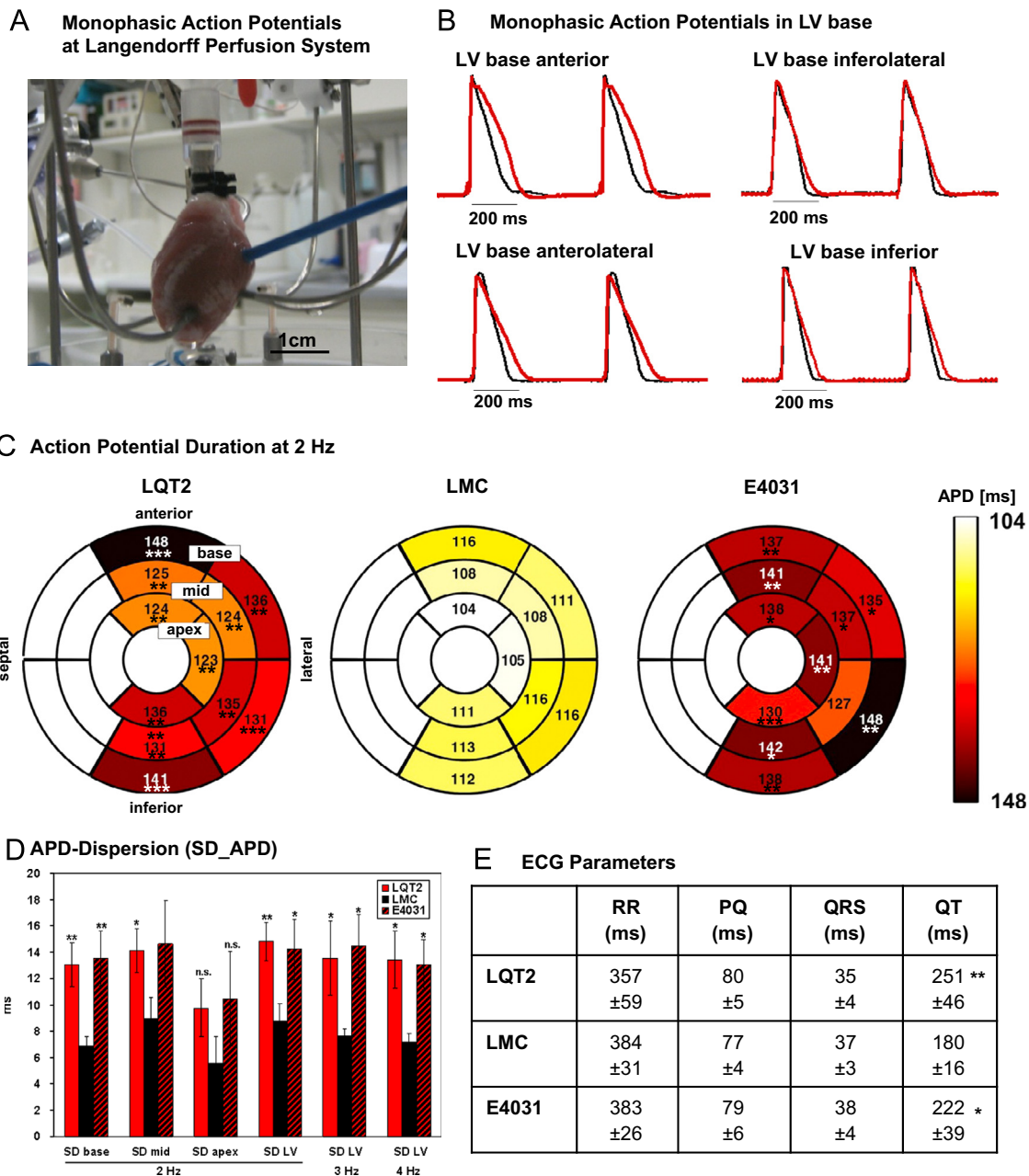
A   Monophasic Action Potentials at Langendorff Perfusion System

B   Monophasic Action Potentials in LV base

LV base anterior   LV base inferolateral

200 ms   200 ms

LV base anterolateral   LV base inferior

200 ms   200 ms

C   Action Potential Duration at 2 Hz

LQT2   LMC   E4031   APD [ms]

D   APD-Dispersion (SD_APD)

E   ECG Parameters

	RR (ms)	PQ (ms)	QRS (ms)	QT (ms)
LQT2	357 ±59	80 ±5	35 ±4	251 ** ±46
LMC	384 ±31	77 ±4	37 ±3	180 ±16
E4031	383 ±26	79 ±6	38 ±4	222 * ±39

Figure 1   Spatial differences in action potential duration. **A:** Langendorff-perfusion setup for MAP measurements. **B:** Representative MAP tracings of individual LQT2 (red) and wild-type littermate control (LMC; black) rabbits. **C:** Bull's eye plots of average APD_{75} (ms). Circles represent (from outside to inside) the LV base, mid, and apex. APDs are color coded as indicated. Septal APDs were not assessed. **D:** APD-dispersion (SD of APD) in the base, mid, apex, and global LV at 2, 3, and 4 Hz. **E:** ECG parameters in LQT2, LMC, and E4031-treated (1 μg/(kg · min)) rabbits. n = 10 LQT2, n = 9 LMC, and n = 10 E4031-treated rabbits; $^*P < .05$, $^{**}P < .01$, $^{***}P < .001$ vs LMC. APD = action potential duration; APD_{75} = action potential duration at 75% of repolarization; ECG = electrocardiogram; LMC = wild-type littermate control; LQT2 = long QT syndrome type 2; LV = left ventricle/ventricular; MAP = monophasic action potential; SD = standard deviation.

base (Figure 5A). Moreover, we could differentiate between E4031-treated and LMC correctly with an accuracy of 100% (see the Online Supplemental Table 3). Most of the relevant features for the classification were regional diastolic Vr and Vz, TTP_dia_Vr, and SDs of Vr_dia, TTP_dia_Vr, and TTP_dia_Vz (see the Online Supplemental Table 2), mainly located in base inferior and mid regions (Figure 5B).

On the basis of the correlations between electrical and mechanical features in LQT2 rabbits, we next tested whether

MRI could provide sufficient information to discern even slight differences in the extent of APD prolongation (LQT2 rabbits with "very long" APD: 164 ± 7.6 ms; LQT2 rabbits with "long" APD: 144 ± 2.8 ms; $P < .001$; see the Online Supplemental Table 1). Using only the 17 most relevant features (see the Online Supplemental Table 2), it was possible to differentiate between "very long" vs "long" APD groups with a classification accuracy of 100% (see the Online Supplemental Table 3). Most relevant features
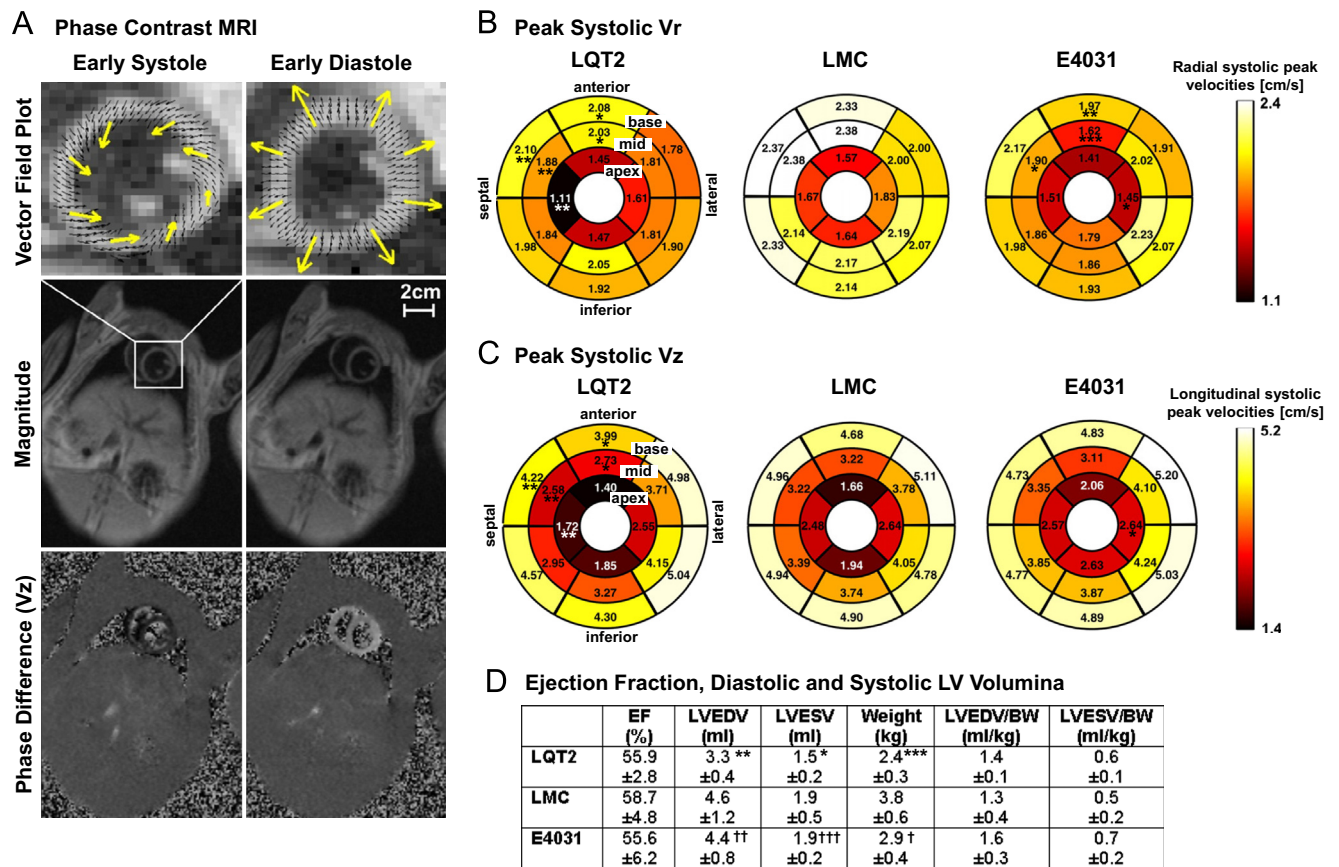
Figure 2 Spatial differences in systolic velocities. **A:** Phase contrast MRI in the LV base during early systole and diastole in representative LMC rabbit. Upper panel: Zoomed vector field plot, with yellow arrows indicating summation vectors. Middle panel: Magnitude images. Square indicates region magnified in the upper panel. Lower panel: Phase difference images containing longitudinal velocity information (Vz). **B:** Bull's eye plots of peak systolic radial velocities (Vr, cm/s). Vr are color coded as indicated. **C:** Bull's eye plots of peak systolic longitudinal velocities (Vz, cm/s). **D:** Ejection fraction (EF) and left ventricular end-diastolic and end-systolic volumes (LVEDV, LVESV). Body-weight-corrected volumes were calculated for better comparison. n = 10 LQT2, n = 9 LMC, and n = 10 E4031-treated rabbits; [*]$P < .05$, [**]$P < .01$, [***]$P < .001$ vs LMC. [†]$P < .05$, [††]$P < .01$, [†††]$P < .001$ vs LQT2. BW = body weight; LMC = wild-type littermate control; LQT2 = long QT syndrome type 2; LV = left ventricle/ventricular; MRI = magnetic resonance imaging; SD = standard deviation.

were diastolic Vr and Vz and TTP_dia-TTP_sys (see the Online Supplemental Table 2), primarily located in the mid (Figure 5C).

Discussion

By using phase contrast MRI, MAP, and multivariate random forest machine learning algorithms, in this study we provide a comprehensive assessment of the regional dispersion of repolarization and mechanical function in LQT2 rabbits. We revealed that a genetically induced or rapid delayed rectifier potassium current (I_{Kr}) blocker-induced prolongation of APD led to a globally and regionally impaired diastolic function and, importantly, that regional differences in APD correlated with regional differences in diastolic dysfunction. These observations indicate that inherited and drug-induced LQTS are not purely electrical but rather electromechanical disorders. Moreover, we demonstrated the possibility to (1) differentiate between LQT2 and normal rabbits and (2) discern differences in the extent of APD prolongation in transgenic LQT2 rabbits solely based on phase contrast MRI data, indicating a potential future use of MRI for risk stratification in LQTS.

Dispersion of repolarization in LQT2 rabbits

A spatially heterogeneous prolongation of repolarization leading to an enhanced APD dispersion is considered a major contributor to LQT-related arrhythmias.[2] LQTS patients have a more pronounced QT and Tpeak-end dispersion, indirectly reflecting regional and transmural APD heterogeneities.[19,20] Spatial and transmural heterogeneities in I_{Kr}, I_{Ks}, and L-type Ca^{2+} current ($I_{Ca,L}$) underlie these pronounced APD heterogeneities in LQTS.[21,22] To directly assess the dispersion of repolarization in LQTS patients, invasive electrophysiological (EPS) studies (EPS) are necessary, and this assessment is limited to regions easily accessible during EPS.[23] Taking advantage of transgenic LQT2 rabbits, we have previously demonstrated a pronounced dispersion of repolarization on right ventricular endocardium[24] and LV anterior surface[9] by using in vivo EPS and ex vivo optical mapping. We here complemented these data by systematically assessing APD in anterior, anterolateral, inferolateral, and inferior regions of the LV base, mid, and apex and demonstrated a more pronounced APD dispersion within each level and global LV. Moreover, we demonstrated that this increased APD dispersion was not altered by faster stimulation despite a rate-dependent APD shortening.
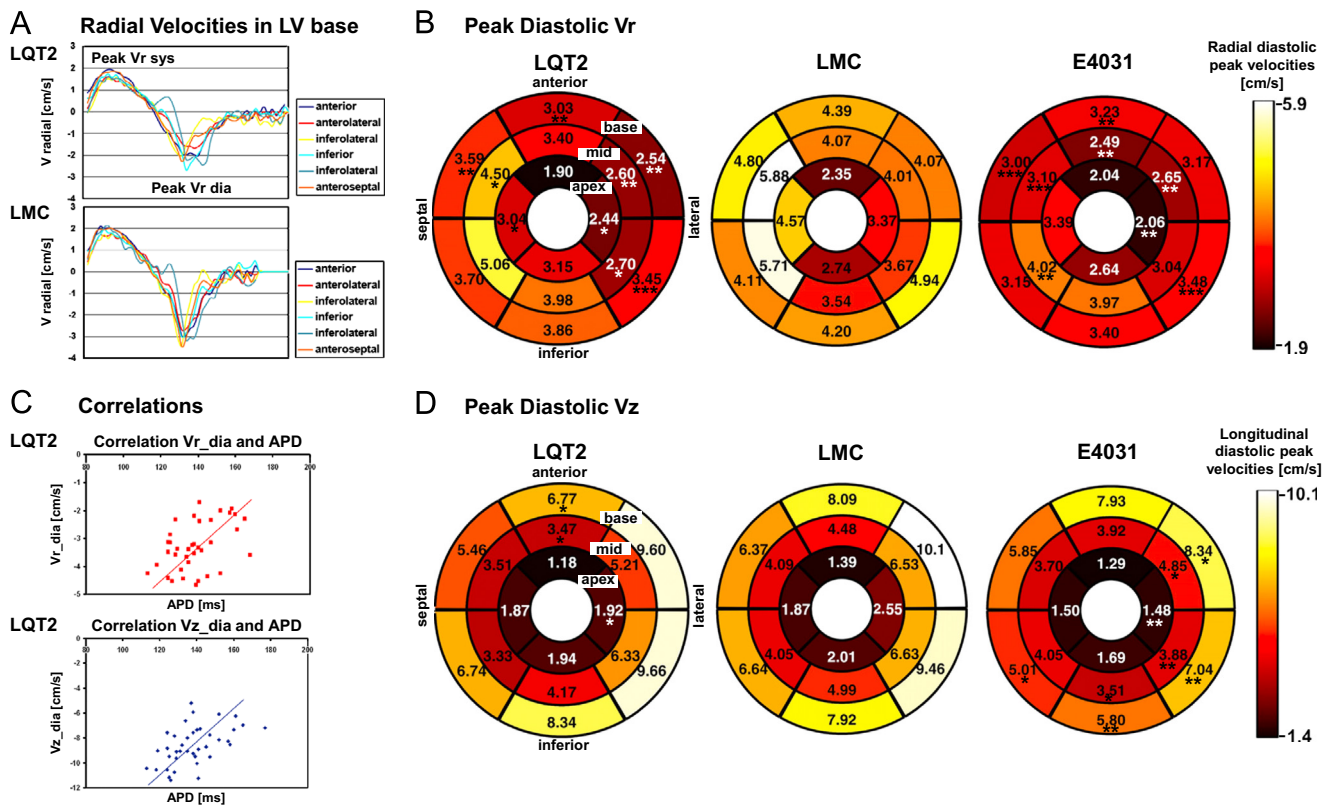
Figure 3   Spatial differences in diastolic velocities. **A:** Graphs of averaged radial velocities (Vr, cm/s) during cardiac cycle (systole: positive values; diastole: negative values) in the LV base in LQT2 (top) and LMC (bottom) rabbits. **B:** Bull's eye plots of peak diastolic radial velocities (Vr, cm/s). Vr are color coded as indicated. **C:** Correlations between APD and reduction in diastolic Vr (top; correlation coefficient [CC] 0.38; $P = .02$) or diastolic long-axis velocities (Vz) in the base (bottom; CC 0.47, $P < .01$) in LQT2 rabbits. **D:** Bull's eye plots of peak diastolic Vz (cm/s). n = 10 LQT2, n = 9 LMC, and n = 10 E4031-treated rabbits; $^*P < .05$, $^{**}P < .01$, $^{***}P < .001$ vs LMC. APD = action potential duration; LMC = wild-type littermate control; LQT2 = long QT syndrome type 2; LV = left ventricle/ventricular; MRI = magnetic resonance imaging; SD = standard deviation.

Dispersion of contractile and diastolic function in LQT2 rabbits

For the first time, we systematically assessed global and regional systolic and diastolic function in LQTS and demonstrated that APD prolongation (1) was associated with delayed cardiac relaxation and (2) had an impact on radial systolic velocities and (3) particularly, on radial and longitudinal diastolic velocities, indicating an impaired mechanical function in LQT2.
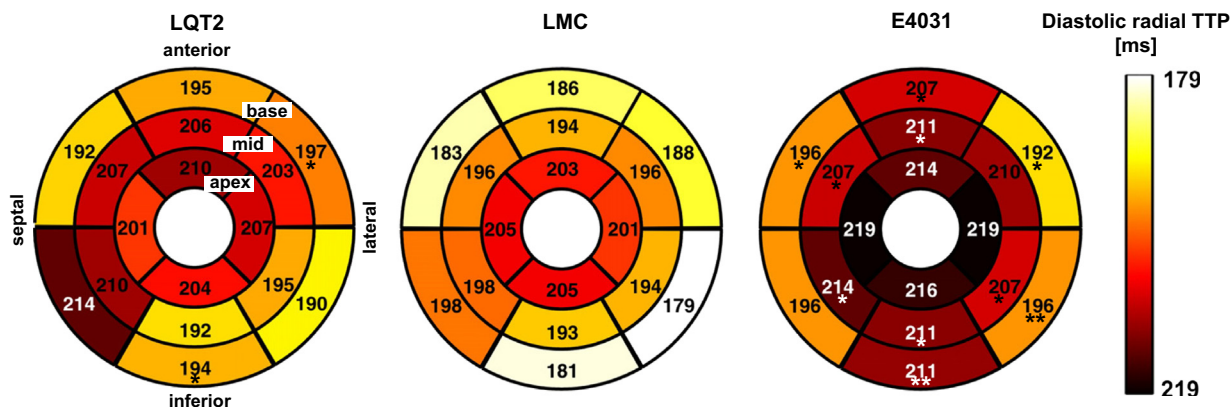
Heart size (LV volumes, ventricular mass, and wall thickness) may affect systolic and less pronouncedly diastolic velocities.[6] The observed pronounced differences in systolic and diastolic velocities in LQT2 and E4031-treated rabbits compared to LMC rabbits, however, cannot (solely) be explained by differences in LV volumes since E4031-treated rabbits were bigger than LQT2 rabbits but had similarly reduced diastolic velocities. Furthermore, differences in heart size cannot explain regional correlations between APD and diastolic velocities in transgenic and drug-induced LQT2 rabbits, as heart size did not vary much within these groups.

Since electrical and mechanical cardiac functions are coupled and affect each other,[25] LQTS patients not only have prolonged repolarization but also have similarly altered v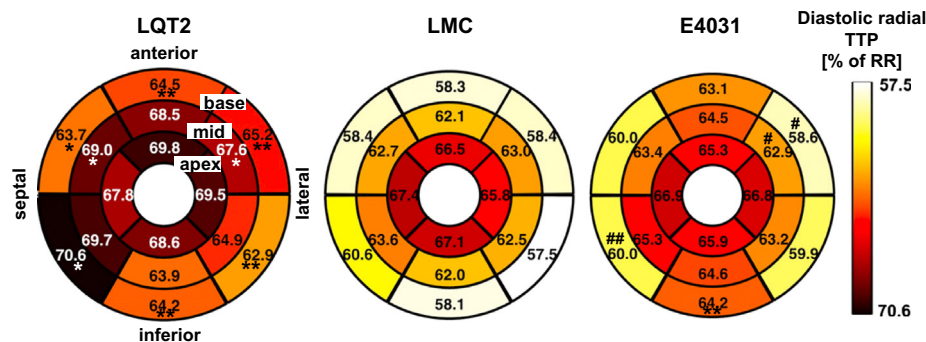entricular contraction patterns with slow contraction in the late wall thickening phase,[26] longer isovolumetric relaxation times,[27] and globally prolonged contraction duration with transmural differences,[3,4] as demonstrated by M-mode and tissue Doppler echocardiography. Moreover, in a case report of an infant with a particularly long QT, the onset of pVTs was preceded by a globally impaired systolic and diastolic function.[28] Two small studies demonstrated that mechanical abnormalities in LQTS patients were associated with arrhythmogenic events[26]: the alteration of myocardial velocities was more sensitive and more specific for the prediction of cardiac events than QTc duration,[3] indicating a possible prognostic value of regional velocity imaging in LQTS patients.

However, the tissue Doppler imaging technique is limited by the low reproducibility and angle dependency of measurements and does not permit the evaluation of all myocardial segments and all velocity directions.[29] Phase contrast MRI overcomes these limitations and allows assessing all velocities in all segments.[5] By using this technique, we revealed that not only global peak velocities are reduced and global time-to-diastolic peak velocities are prolonged in LQT2, but also that the reduction of diastolic velocities and prolongation of contraction duration are regionally heterogeneous, indicating a mechanical dispersion. Interestingly, in transgenic LQT2 rabbits, Vr were particularly reduced and radial
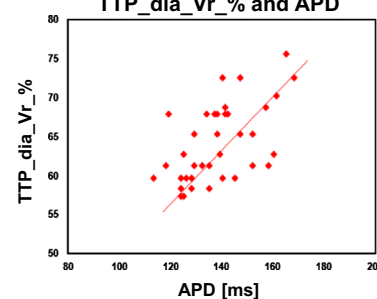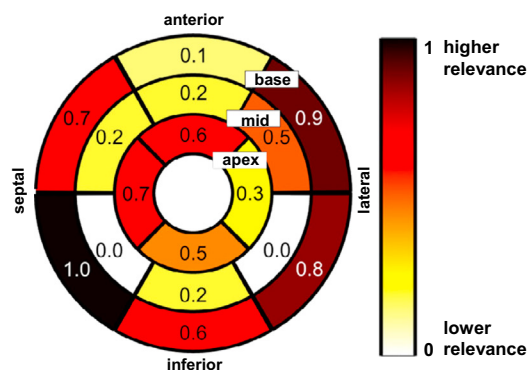
Figure 4 Differences in time-to-diastolic peak velocities. **A:** Bull's eye plots of time-to-diastolic peak radial velocities (TTP_dia_Vr, ms). TTP are color coded as indicated. **B:** Bull's eye plots of heart-rate corrected TTP_diastolic_% in Vr. **C:** Correlation between APD and time-to-diastolic peak Vr in the base (correlation coefficient [CC] 0.47; $P = .001$) in LQT2 rabbits. n = 10 LQT2, n = 9 LMC, and n = 10 E4031-treated rabbits; [*]$P < .05$, [**]$P < .01$ vs LMC; [#]$P < .05$, [##]$P < .01$ vs LQT2. APD = action potential duration; LMC = wild-type littermate control; LQT2 = long QT syndrome type 2; LV = left ventricle/ventricular; SD = standard deviation; Vr = radial velocities; Vz = long-axis velocities.
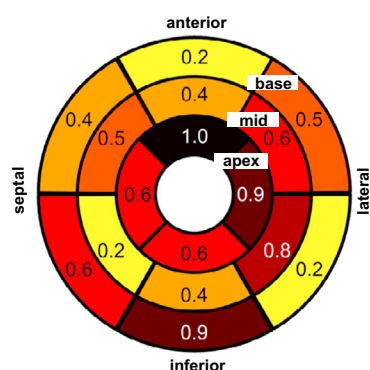
time-to-diastolic peak was particularly prolonged. In line with our findings, in LQTS patients, a very slow late contraction was observed in radial direction.[26] Moreover, dispersion parameters and contraction duration in Vr demonstrated the highest correlations with APD. These observations stress the particular importance of evaluating regional radial motion in LQTS, which cannot be assessed in all LV segments by using standard echocardiography.
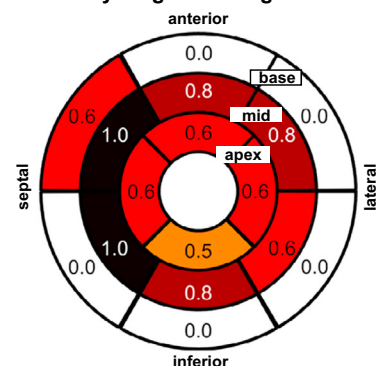

Figure 5 Classification based on phase contrast MRI. **A:** Bull's eyes plot of cumulative region relevance for LQT2 vs LMC classification. Chi-square attribute values of most relevant features were added within each region, normalized, and color coded as indicated. None of the relevant features were located in white regions. **B:** Bull's eyes plot of cumulative region relevance for E4031 vs LMC classification. **C:** Bull's eyes plot of cumulative region relevance for "very long" vs "long" APD classification. APD = action potential duration; LMC = wild-type littermate control; LQT2 = long QT syndrome type 2; LV = left ventricle/ventricular; MRI = magnetic resonance imaging.

Correlation of electrical and mechanical dysfunction and MRI-based differentiation of electrical phenotype

Although it has previously been shown that LQTS patients have a pronounced dispersion of both cardiac repolarization and (transmural) contraction duration[4] thus far, no study has investigated a potential spatial relationship between electrical and mechanical dispersion in LQTS. Taking advantage of transgenic LQT2 rabbits,[9] in which mechanical and electrical function can be assessed systematically in similar segments, we revealed for the first time a spatial correlation between APD and the extent of diastolic dysfunction, contraction duration, and mechanical dispersion, indicating a close coupling of spatially heterogeneous electrical and mechanical dysfunction in LQTS. Owing to electromechanical coupling in cardiomyocytes, one might expect an even stronger statistical correlation than the one observed in our study. However, regional differences in fiber orientation and heart geometry at different segments may also affect amplitude and timing of radial, longitudinal, and rotational velocities, thus modulating the direct effect of APD on relaxation characteristics. Nevertheless, this observed correlation between electrical and mechanical changes in LQT2 rabbits was pronounced enough to discern even moderate differences in the extent of APD prolongation solely based on phase contrast MRI data.

How this altered electromechanical function in LQTS may affect arrhythmogenesis, for example, via reverse excitation-contraction coupling,[25] via activation of stretch-sensible ion channels,[30] or via reduced coronary perfusion due to prolonged cardiac contraction and impaired diastolic relaxation, remains to be elucidated. APD prolongation results in increased Ca^{2+} influx via $I_{Ca,L}$ and increased Ca^{2+}-induced Ca^{2+}-release from the sarcoplasmic reticulum, thus increasing cytoplasmic Ca^{2+} concentration ($[Ca^{2+}]_i$).[31] Since physical properties of (resting) sarcomeres are related to $[Ca^{2+}]_i$,[32] an increased $[Ca^{2+}]_i$ may result in an impaired diastolic relaxation. Moreover, the increased $[Ca^{2+}]_i$ should also increase systolic function.[31] However, our data suggest that systolic function in LQT2 hearts is decreased, which is indicative of a complex remodeling of Ca^{2+} handling systems like an adaptive decrease in $I_{Ca,L}$ density observed in transgenic LQT2 rabbits.[33] Further studies are necessary to fully characterize molecular mechanisms responsible for adaptive changes contributing to systolic and diastolic dysfunction in LQT2.

Clinical implications

To date, LQTS is mainly considered an "electrical" disorder, in which QTc duration[18] and QT dispersion[19] are known arrhythmogenic risk predictors. The facts (1) that regional differences in APD correlate with regional differences in diastolic dysfunction and (2) that it is possible to discern differences in the extent of APD prolongation by using phase contrast MRI might open new approaches for risk stratification and treatment decisions of LQTS patients. In the future,

it might be possible to use phase contrast MRI to assess the arrhythmogenic risk in LQTS patients noninvasively by deducing electrical dispersion from segmental mechanical function and dispersion.

Transgenic LQT2 rabbits overexpress the dominant-negative loss-of-function mutation HERG-G628S, which leads to a complete loss of I_{Kr}. Many missense mutations in HERG in LQT2 patients, however, lead to a substantial decrease rather than a complete loss of I_{Kr}. The findings of pronounced diastolic dysfunction in transgenic LQT2 rabbits thus likely recapitulate findings in human patients with a (complete) loss of functional I_{Kr}. The fact that I_{Kr}-blocker E4031, which only reduces I_{Kr}, also induces diastolic abnormalities, however, indicates that LQT2 patients with a substantial decrease in I_{Kr} may have similar diastolic dysfunction.

To validate the potential use of phase contrast MRI for risk stratification, further studies investigating its potential to predict the development of pVTs and clinical pilot studies investigating the extent of mechanical (dys)function and its spatial dispersion in LQTS patients with different mutations, different QTc durations, and different arrhythmia incidences are certainly warranted.

Study limitations

Regional mechanical and electrical data were acquired in different experimental settings, for example, in vivo MRI and ex vivo MAP in Langendorff-perfused hearts. Ideally, both should be assessed simultaneously in the same in vivo setting to perfectly correlate regional mechanical and electrical functions. However, to date, detailed segmental MAP measurements are not feasible in an in vivo setting and it is still challenging to obtain any—let alone detailed—regional electrical data during MRI.

The "diastolic dysfunction," for example, abnormal cardiac relaxation, observed in LQT2 rabbits must be differentiated from "diastolic heart failure." Clinically, none of the LQT2 rabbits showed any signs of diastolic heart failure, similarly as in LQTS patients, in whom no clinical signs of heart failure were reported, even in older patients or in patients with particularly prolonged QT.[34] Moreover, so far, none of the clinical manifestations of LQTS has been directly, pathophysiologically linked to the presence of severe mechanical dysfunction. Importantly, however, we could demonstrate that mechanical cardiac function was sufficiently altered in LQT2 to allow a differentiation between LQT2 and normal hearts solely based on phase contrast MRI data. These data indicate that LQTS should probably be considered not only an electrical disorder but rather an electromechanical disorder.

Conclusions

Prolongation and increased dispersion of cardiac repolarization led to globally and regionally impaired diastolic and systolic mechanical function and increased mechanical dispersion in transgenic and drug-induced LQT2 rabbits.

Moreover, in transgenic LQT2 rabbits, regional differences in APD correlated with the extent of reduction of regional diastolic peak velocities and regional time-to-diastolic peak velocities – as marker of impaired diastolic function, indicating that LQTS is not purely an electrical but rather an electromechanical disorder. Finally, due to this association of electrical and mechanical functions, it was possible to (1) differentiate between LQT2 and normal LMC rabbits' hearts, and to (2) discern differences in the extent of APD prolongation and APD dispersion in LQT2 rabbits solely based on MRI data, indicating potential new approaches for risk stratification and treatment decisions of LQTS patients.

Acknowledgments

Appendix
Supplementary data

Supplementary data associated with this article can be found in the online version at http://dx.doi.org/10.1016/j.hrthm.2013.07.038.

References

1. Roden DM. Clinical practice: long-QT syndrome. N Engl J Med 2003;358:169–176.
2. Antzelevitch C. Role of spatial dispersion of repolarization in inherited and acquired sudden cardiac death syndromes. Am J Physiol Heart Circ Physiol 2007;293:H2024–H2038.
3. Haugaa KH, Edvardsen T, Leren TP, Gran JM, Smiseth OA, Amlie JP. Left ventricular mechanical dispersion by tissue Doppler imaging: a novel approach for identifying high-risk individuals with long QT syndrome. Eur Heart J 2009;30:330–337.
4. Haugaa KH, Amlie JP, Berge KE, Leren TP, Smiseth OA, Edvardsen T. Transmural differences in myocardial contraction in long-QT syndrome: mechanical consequences of ion channel dysfunction. Circulation 2010;122:1355–1363.
5. Jung B, Föll D, Böttler P, Petersen S, Hennig J, Markl M. Detailed analysis of myocardial motion in volunteers and patients using high-temporal-resolution MR tissue phase mapping. J Magn Reson Imaging 2006;24:1033–1039.
6. Föll D, Jung B, Schilli E, et al. Magnetic resonance tissue phase mapping of myocardial motion: new insight in age and gender. Circ Cardiovasc Imaging 2010;3:54–64.
7. Nerbonne JM. Molecular basis of functional voltage-gated K^+ channel diversity in the mammalian myocardium. J Physiol 2000;525:285–298.
8. Bers DM. Cardiac Na/Ca exchange function in rabbit, mouse and man: what's the difference? J Mol Cell Cardiol 2002;34:369–373.
9. Brunner M, Peng X, Liu GX, et al. Mechanisms of cardiac arrhythmias and sudden death in transgenic rabbits with long QT syndrome. J Clin Invest 2008;118:2246–2259.
10. Ripplinger CM, Li W, Hadley J, et al. Enhanced transmural fiber rotation and connexin 43 heterogeneity are associated with an increased upper limit of vulnerability in a transgenic rabbit model of human hypertrophic cardiomyopathy. Circ Res 2007;101:1049–1057.
11. Jung BA, Odening KE, Dall'Armellina E, Foell D, Markl M, Schneider J. A comprehensive quantitative comparison of regional myocardial motion in mice, rabbits and humans using phase contrast MRI. J Cardiovasc Magn Reson Imaging 2012;14:87.
12. Michael G, Dempster J, Kane KA, Coker SJ. Potentiation of E-4031-induced torsade de pointes by HMR1556 or ATX-II is not predicted by action potential short-term variability or triangulation. Br J Pharmacol 2007;152:1215–1227.
13. Odening KE, Hyder O, Chaves L, et al. Pharmacogenomics of anesthetic drugs in transgenic LQT1 and LQT2 rabbits reveal genotype-specific differential effects on cardiac repolarization. Am J Physiol Heart Circ Physiol 2008;295:H2264–H2272.
14. Cerqueira MD, Weissman NJ, Dilsizian V, et al. Standardized myocardial segmentation and nomenclature for tomographic imaging of the heart: a statement for healthcare professionals from the Cardiac Imaging Committee of the Council on Clinical Cardiology of the American Heart Association. Circulation 2002;105:539–542.
15. D'Alonzo AJ, Zhu JL, Darbenzio RB. Effects of class III antiarrhythmic agents in an in vitro rabbit model of spontaneous torsades de pointe. Eur J Pharmacol 1999;369:57–64.
16. Bentzen BH, Bahrke S, Wu K, et al. Pharmacological activation of Kv11.1 in transgenic long QT-1 rabbits. J Cardiovasc Pharmacol 2011;57:223–230.
17. Menze BH, Kelm BM, Masuch R, et al. A comparison of random forest and its Gini importance with standard chemometric methods for the feature selection and classification of spectral data. BMC Bioinformatics 2009;10:213–229.
18. Sauer AJ, Moss AJ, McNitt S, et al. Long QT syndrome in adults. J Am Coll Cardiol 2007;49:329–337.
19. Priori SG, Napolitano C, Diehl L, Schwartz PJ. Dispersion of the QT interval: a marker of therapeutic efficacy in the idiopathic long QT syndrome. Circulation 1994;89:1681–1689.
20. Lubinski A, Lewicka-Nowak E, Kempa M, Baczynska AM, Romoanowska I, Swiatecka G. New insight into repolarization abnormalities in patients with congenital long QT syndrome: the increased transmural dispersion of repolarization. Pacing Clin Electrophysiol 1998;21:172–175.
21. Cheng J, Kamiya K, Liu W, Tsuji Y, Toyama J, Kodama I. Heterogeneous distribution of the two components of delayed rectifier K^+ current: a potential mechanism of the proarrhythmic effects of methanesulfonanilideclass III agents. Cardiovasc Res 1999;43:135–147.
22. Pham TV, Robinson RB, Danilo P, Jr, Rosen MR. Effects of gonadal steroids on gender-related differences in transmural dispersion of L-type calcium current. Cardiovasc Res 2002;53:752–762.
23. Bhandari AK, Shapiro WA, Morady F, Shen EN, Mason J, Scheinman MM. Electrophysiologic testing in patients with the long-QT syndrome. Circulation 1985;71:63–71.
24. Odening KE, Kirk M, Brunner M, et al. Electrophysiological studies of transgenic long QT type 1 and type 2 rabbits reveal genotype-specific differences in ventricular refractoriness and His conduction. Am J Physiol Heart Circ Physiol 2010;299:H643–H655.
25. Ter Keurs HE. Electromechanical coupling in the cardiac myocyte: stretch-arrhythmia feedback. Plugers Arch 2011;462:165–175.
26. Nador F, Beria G, De Ferrari GM, et al. Unsuspected echocardiographic abnormality in the long QT syndrome: diagnostic, prognostic, and pathogenetic implications. Circulation 1991;84:1530–1542.
27. Savoye C, Klug D, Denjoy I, et al. Tissue Doppler echocardiography in patients with long QT syndrome. Eur J Echocardiogr 2003;4:209–213.
28. Vyas H, O'Leary PW, Earing MG, Cetta T, Ackerman MJ. Mechanical dysfunction in extreme QT prolongation. J Am Soc Echocardiogr 2008;21:511:e15–e17.
29. Thibault H, Derumeaux G. Assessment of myocardial ischemia and viability using tissue Doppler and deformation imaging: the lessons from experimental studies. Arch Cardiovasc Dis 2008;101:61–68.
30. Wang Y, Joyner RW, Wagner MB, Cheng J, Lai D, Crawford BH. Stretch-activated channel activation promotes early afterdepolarizations in rat ventricular myocytes under oxidative stress. Am J Physiol Heart Circ Physiol 2009;296:H1227–H1235.
31. Bassani RA. Transient outward potassium current and Ca^{2+} homeostasis in the heart: beyond the action potential. Braz J Med Biol Res 2006;39:393–403.
32. Stuyvers BD, Miura M, ter Keurs HE. Ca(2+)-dependence of passive properties of cardiac sarcomeres. Adv Exp Med Biol 2000;481:353–366.
33. Liu GX, Choi BR, Ziv O, et al. Differential conditions for early after-depolarizations and triggered activity in cardiomyocytes derived from transgenic LQT1 and LQT2 rabbits. J Physiol 2012;590:1171–1180.
34. Goldenberg I, Moss AJ, Bradley J, et al. Long-QT syndrome after age 40. Circulation 2008;117:2192–2201.